Measurement of ^2H T_1 and $T_{1\rho}$ Relaxation Times in Uniformly ^{13}C-Labeled and Fractionally ^2H-Labeled Proteins in Solution

D. R. Muhandiram,† Toshio Yamazaki,† Brian D. Sykes,‡ and Lewis E. Kay*,†

Contribution from the Protein Engineering Centers of Excellence and Departments of Medical Genetics, Biochemistry, and Chemistry, University of Toronto, Toronto, Ontario, Canada M5S 1A8, and Protein Engineering Centers of Excellence, Department of Biochemistry, and MRC Group in Protein Structure and Function, University of Alberta, Edmonton, Alberta, Canada T6G 2H7

Received June 21, 1995®

Abstract: A novel method is presented for the measurement of relaxation properties of methyl group deuterons in proteins uniformly ^{13}C labeled and fractionally deuterated. The experiments select for $^{13}CH_2D$ methyl groups and make use of the excellent resolution provided by constant time $^{13}C-^1H$ correlation spectroscopy to measure the ^2H relaxation rates, $1/T_1$ and $1/T_{1\rho}$, at all methyl positions in the protein. Since the relaxation of a deuteron is completely dominated by the quadrupolar interaction, interpretation of the relaxation data is more straightforward than is the case for relaxation data from other nuclei, where the relaxation rates often contain contributions from a number of interactions. The experiments are applied to study the sidechain dynamics of the C-terminal SH2 domain from phospholipase $C_{\gamma 1}$.

Introduction

Recently it has been demonstrated that the use of fractional deuteration in concert with uniform ^{15}N and ^{13}C labeling of proteins is an important strategy in extending the molecular weight limitations of present NMR methods.[1-3] In contrast to the relatively recent resurgence of interest in the use of deuteration for high-resolution macromolecular NMR studies,[1-8] ^2H NMR spectroscopy has enjoyed a rich history in the study of molecular dynamics through measurements of ^2H relaxation and/or line shape parameters.[9] Efforts in this regard have principally focused on the use of liquid crystalline samples or samples in the solid state. Herein we report, for the first time, methods for measuring ^2H relaxation properties of methyl group deuterons in proteins dissolved in solution and labeled uniformly with ^{13}C and fractionally with deuterium. Relaxation studies of proteins, to date, have concentrated primarily on backbone dynamics.[10] However, an understanding of sidechain motions in proteins is of potentially greater interest. Methyl groups are a particularly good target for dynamics studies because of their high frequency of occurrence in proteins coupled with their distribution at various positions in relation to the protein backbone. The experiments proposed select specifically for $^{13}CH_2D$ methyl groups and make use of the high resolution provided by constant-time $^{13}C-^1H$ correlation spectroscopy[11,12] to measure the deuterium relaxation rates at all methyl positions in the protein. Because the relaxation of a deuteron is dominated by the quadrupolar interaction, the interpretation of the relaxation data is more straightforward than is the case for relaxation data from many other nuclei.

The methods developed are applied to study the sidechain dynamics of the C-terminal SH2 domain from phospholipase $C_{\gamma 1}$ (PLCC SH2). A recent ^{15}N backbone dynamics study by Farrow *et al.*[13] noted that upon binding phosphorylated peptide few changes in order parameters were observed, indicating that nanosecond/picosecond motion along the protein backbone remains relatively unchanged. However, based on the refined structure of the complex,[14] it is clear that a large number of sidechains participate in crucial interactions with the peptide. It is of interest to examine how sidechain mobility might be altered upon binding and whether residues that are key to the binding process are unusually flexible in the free state to accommodate the large number of phosphorylated peptide sequences that can bind to this particular SH2 domain.[15] In the present paper, we describe the methodology that has been developed and establish that the approach for obtaining the

† University of Toronto.
‡ University of Alberta.
® Abstract published in *Advance ACS Abstracts*, October 15, 1995.

(1) Grzesiek, S.; Anglister, J.; Ren, H.; Bax, A. *J. Am. Chem. Soc.* **1993**, *115*, 4369.
(2) Yamazaki, T.; Lee, W.; Revington, M.; Mattiello, D. L.; Dahlquist, F. W.; Arrowsmith, C. H.; Kay, L. E. *J. Am. Chem. Soc.* **1994**, *116*, 6464.
(3) (a) Yamazaki, T.; Lee, W.; Arrowsmith, C. H.; Muhandiram, D. R.; Kay, L. E. *J. Am. Chem. Soc.* **1994**, *116*, 11655. (b) Farmer, B. T., II; Venters, R. A. *J. Am. Chem. Soc.* **1995**, *117*, 4187.
(4) Kushlan, D. M.; LeMaster, D. M. *J. Biomol. NMR* **1993**, *3*, 701.
(5) LeMaster, D. M.; Richards, F. M. *Biochemistry* **1988**, *27*, 142.
(6) Shon, K. J.; Opella, S. J. *Science* **1991**, *252*, 1303.
(7) Arrowsmith, C. H.; Pachter, R.; Altman, R. B.; Iyer, S. B.; Jardetzky, O. *Biochemistry* **1990**, *29*, 6332.
(8) Zhang, H.; Zhao, D.; Revington, M.; Lee, W.; Jia, X.; Arrowsmith, C. H.; Jardetzky, O. *J. Mol. Biol.* **1994**, *229*, 735.
(9) (a) Jelinski, L. W.; Sullivan, C. E.; Torchia, D. A. *Nature (London)* **1980**, *284*, 531. (b) Seelig, J. *Q. Rev. Biophys.* **1977**, *10*, 353. (c) Keniry, M. A.; Rothget, M.; Smith, R. L.; Gutowsky, H. S.; Oldfield, E. *Biochemistry* **1983**, *22*, 1917. (d) Vold, R. R.; Vold, R. L. *Adv. Magn. Reson.* **1991**, *16*, 85.
(10) (a) Kay, L. E.; Torchia, D. A.; Bax, A. *Biochemistry* **1989**, *28*, 8972. (b) Clore, G. M.; Driscoll, P. C.; Wingfield, P. T.; Gronenborn, A. *Biochemistry* **1990**, *29*, 7387. (c) Stone, M. J.; Fairbrother, W. J.; Palmer, A. G.; Reizer, J.; Saier, M. H.; Wright, P. E. *Biochemistry* **1992**, *31*, 4394. (d) Kordel, J.; Skelton, N. J.; Akke, M.; Palmer, A. G.; Chazin, W. J. *Biochemistry* **1992**, *31*, 4856. (e) Peng, J. W.; Wagner, G. *Biochemistry* **1992**, *31*, 8571. (f) Nicholson, L. K.; Yamazaki, T.; Torchia, D. A.; Grzesiek, S.; Bax, A.; Stahl, S. J.; Kaufman, J. D.; Wingfield, P. T.; Lam, P. Y.; Jadhav, P. K.; Hodge, C. N.; Domaille, P. J.; Chang, C. H. *Nature Struct. Biol.* **1995**, *2*, 274.
(11) Santoro, J.; King, G. C. *J. Magn. Reson.* **1992**, *97*, 202.
(12) Vuister, G. W.; Bax, A. *J. Magn. Reson.* **1992**, *101*, 201.
(13) Farrow, N. A.; Muhandiram, D. R.; Singer, A. U.; Pascal, S. M.; Kay, C. M.; Gish, G.; Shoelson, S. E.; Pawson, T.; Forman-Kay, J. D.; Kay, L. E. *Biochemistry* **1994**, *33*, 5984.
(14) (a) Pascal, S. M.; Singer, A. U.; Gish, G.; Yamazaki, T.; Shoelson, S. E.; Pawson, T.; Kay, L. E.; Forman-Kay, J. D. *Cell* **1994**, *77*, 461. (b) Pascal, S. M.; Singer, A. U.; Pawson, T.; Kay, L. E.; Forman-Kay, J. D. In preparation.

0002-7863/95/1517-11536$09.00/0

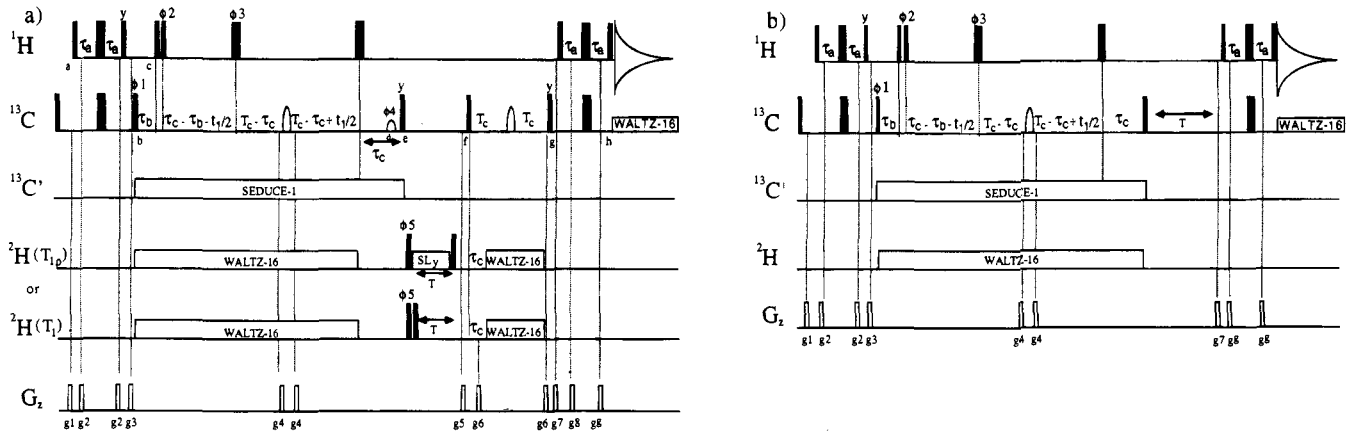

Figure 1. (a) Pulse schemes to measure $T_{1\rho}(I_zC_zD_y)$ or $T_1(I_zC_zD_z)$ values in $^{13}CH_2D$ spin systems. All narrow (wide) rectangular pulses are applied with a flip angle of 90° (180°). The carriers are centered at 4.7, 20.0, and 0.8 ppm for ^1H, ^{13}C, and ^2H, respectively. All ^1H pulses are applied using a 23.8-kHz field while the ^{13}C rectangular pulses are applied with a 19.2-kHz field. The two shaped ^{13}C 180° pulses, applied in the middle of periods b−e and f−g, are 360-μs RE-BURP[28] pulses (17.3-kHz field at maximum intensity) with the excitation maximum centered at 35 ppm via phase modulation of the rf.[29,30] The $^{13}C^\alpha$ selective 90° pulse at point d is applied as a 690-μs pulse having the SEDUCE-1[31] profile with an excitation maximum centered at 57.5 ppm. Carbon decoupling during acquisition is achieved using a 2.1-kHz WALTZ-16 field;[32] carbonyl decoupling is performed using a 158-ppm cosine-modulated WALTZ-16 sequence[33] employing pulses having the SEDUCE-1 shape (345 μs 90° pulse width). A 790-Hz WALTZ-16 field was applied for ^2H decoupling, a 1.05-kHz ^2H spin-lock field (SL_y) was employed in the $T_{1\rho}$ experiment, and a 2.3-kHz field was used for ^2H 90° pulses. The delays employed are as follows: $\tau_a = 1.7$ ms, $\tau_b = 3.85$ ms, $\tau_c = 11.0$ ms, $T_C = 14.5$ ms. Repetition delays of 1.8 s in the T_1 experiment and 2.0 s in the $T_{1\rho}$ experiment were employed. The phase cycling used is as follows: $\phi1 = 8(x), 8(-x)$; $\phi2 = (x,-x)$; $\phi3 = 2(x), 2(-x)$; $\phi4 = 16(x), 16(-x)$; $\phi5 = 4(x), 4(-x)$; acq $= 2(x,-x), 4(-x,x), 2(x,-x)$. Quadrature in F_1 is achieved via States-TPPI[16] of $\phi1$. The durations and strengths of the gradients are as follows: g1 = (0.5 ms, 5 G/cm), g2 = (0.3 ms, 3 G/cm), g3 = (1.5 ms, 15 G/cm), g4 = (0.3 ms, 25 G/cm), g5 = (0.4 ms, −10G/cm), g6 = (0.2 ms, −10 G/cm), g7 = (1.0 ms, −15 G/cm), g8 = (0.3 ms, 2 G/cm). All experiments can be performed in H_2O with excellent solvent suppression. In order to ensure that the effects of the gradients g3, g4, g5, g6, and g7 are additive with respect to dephasing of water (and artifacts), the sign of the gradients g4, g5, g6, and g7 is changed in concert with alternation of the rf phase $\phi2$. The values of the gradients indicated correspond to the $\phi2 = x$ case. A delay of 10 ms is inserted after the application of the final ^{13}C 90° pulse (phase y) to allow the lock to stabilize. The strong gradient g7 applied during this time ensures that all ^2H magnetization (from D_2O) in the transverse plane is completely dephased when the lock is resampled, thus improving the stability further. Decoupling is interrupted during application of the gradient pulses. (b) Pulse scheme for measuring $T_1(I_zC_z)$. Details of the experiment are the same as described in (a) with the exception that the phase cycling is $\phi1 = 4(x), 4(-x)$; $\phi2 = (x,-x)$; $\phi3 = 2(x), 2(-x)$; acq $= 2(x,-x), 2(-x,x)$.

deuterium T_1 and $T_{1\rho}$ values, T_1(D) and $T_{1\rho}$(D), is theoretically sound. Of necessity this requires a mathematical treatment; however, as demonstrated below the method is very simple to use and the interpretation of the resultant relaxation data straightforward. Finally, T_1 and $T_{1\rho}$ results from a relaxation study of the PLCC SH2 domain are presented.

Experimental Section

^{15}N,^{13}C fractionally deuterated PLCC SH2 was expressed in *E. coli* BL21 cells grown at 30 °C in M9 minimal media, 65% D_2O, 35% H_2O, with $^{15}NH_4Cl$ (1 g per L of culture) and $^{13}C_6$-glucose (3 g per L of culture) as the sole nitrogen and carbon sources. The details of the purification are as described previously.[13,14] Editing experiments which select for nonprotonated (i.e., CD or CD_2) carbons adjacent to methyl groups have established levels of deuteration of approximately 55% at the C^α position of Ala residues and 45−55% for sidechain carbons.

NMR experiments were performed on a 1.5 mM sample, pH 6.4, 90% H_2O, 10% D_2O, 30 °C. The ^2H T_1 and $T_{1\rho}$ relaxation experiments were implemented on both Varian UNITY+ 600 and 500 MHz spectrometers equipped with pulsed field gradient units and actively shielded probeheads. The ^2H lock receiver was disabled immediately prior to the application of the first pulse and activated prior to acquisition in the pulse schemes described in Figures 1 and 6.

$T_1(I_zC_zD_z)$ values were measured from nine 2D spectra recorded with T delays of 0.05, 4.5, 9.5, 15, 21, 28, 36, 45, and 57.7 ms. Values of $T_1(I_zC_z)$ were obtained using identical T delays. $T_1(I_zC_zD_y)$ values were based on eight 2D spectra recorded using a 1.05 kHz spin lock field with delays of 0.20, 1.3, 2.8, 4.4, 6.2, 8.4, 10.9, and 15.1 ms. All data sets were recorded as 76 × 576 complex matrices using the pulse schemes of Figure 1. Quadrature was obtained in t_1 using States-TPPI.[16] All spectra were processed and analyzed using routines in nmrPipe.[17] Cross peak intensities were fit to a function of the form $I(T) = I(0)\exp(-T/T_i)$, where $1/T_i$ is the relevant relaxation rate and $I(T)$ is the intensity of a given cross peak at time T. No evidence of multiexponential decay of the data was observed. Errors in measured relaxation rates were estimated using Monte Carlo procedures discussed in detail elsewhere[13] and were, on average, 4% of the measured values. Motional parameters were extracted using a form of the spectral density function described in detail below, by minimizing the function

$$\chi^2 = \sum[(T_1^{\,c} - T_1^{\,e})^2/\sigma_{T_1}^{\,2} + (T_{1\rho}^{\,c} - T_{1\rho}^{\,e})^2/\sigma_{T_{1\rho}}^{\,2}] \quad (1)$$

where the superscripts c and e refer to calculated and experimentally determined relaxation parameters, respectively, σ_{T_i} is the estimate of the standard deviation of the experimentally determined parameter, T_i, and the summation is over data obtained at both 500 and 600 MHz.

Results and Discussion

Figures 1a,b illustrate the pulse schemes that were developed to measure ^2H $T_{1\rho}$ and T_1 relaxation times. The methods build upon constant-time $^1H-^{13}C$ HSQC sequences that have been proposed to measure (^{13}C,^1H) correlations and therefore only a brief description of the magnetization transfer pathway is provided. In what follows the sequence of Figure 1a is described. Magnetization originating on protons at point a in the pulse scheme is transferred via INEPT[18] to the attached ^{13}C

(15) (a) Songyang, Z.; Shoelson, S. E.; Chauduri, M.; Gish, G.; Pawson, T.; Haser, W. G.; King, F.; Roberts, T.; Ratnofsky, S.; Lechleider, R. J.; Neel, B. G.; Birge, R. B.; Fajardo, J. E.; Chou, M. M.; Hanafusa, H.; Schaffhausen, B.; Cantley, L. C. *Cell* **1993**, *72*, 767. (b) Rotin, D.; Margolis, B.; Mohammadi, M.; Daly, R. J.; Daum, G.; Li, N.; Fischer, E. H.; Burgess, W. H.; Ullrich, A.; Schlessinger, J. *EMBO J.* **1992**, *11*, 559.

(16) Marion, D.; Ikura, M.; Tschudin, R.; Bax, A. *J. Magn. Reson.* **1989**, *85*, 393.

(17) Delaglio, F. nmrPipe System of Software; National Institutes of Health; Bethesda, MD, 1993.

(18) Morris, G. A.; Freeman, R. *J. Am. Chem. Soc.* **1979**, *101*, 760.

spin. Subsequently ^{13}C magnetization is allowed to evolve for a period $\tau_b = 1/(2J_{CH})$. At this point the magnetization associated with $^{13}CH_3$, $^{13}CHD_2$, and $^{13}CH_2D$ groups is given by operator terms of the form $C_{TR}I_z^iI_z^j$ ($i \neq j$), C_{TR}, $C_{TR}I_z$, respectively, where C_{TR} denotes transverse carbon magnetization, I_z^i, I_z^j represent the z components of magnetization associated with methyl proton spins i and j respectively, and $I_z = I_z^i + I_z^j$. Application of the ^1H $90_x90_{\phi 2}$ pulse pair at point c in the sequence, with the phase $\phi 2$ inverted on alternate scans, changes the sign of the signal originating from $^{13}CH_2D$ methyl groups every second scan, while magnetization associated with either $^{13}CH_3$ or $^{13}CHD_2$ methyls remains unchanged. Selection for signals from $^{13}CH_2D$ groups exclusively is achieved, therefore, by inverting the phase $\phi 2$ and the phase of the receiver in concert.

The ^{13}C chemical shift is recorded in a constant-time manner during the delay $2T_C = 1/J_{CC}$ (J_{CC} is the one bond carbon carbon coupling constant), from points b to e in Figure 1a. At $\tau_c \sim 1/(4J_{CD})$ prior to point e, where J_{CD} is the value of the one-bond $^{13}C-^2H$ scalar coupling, ^2H decoupling is terminated and evolution of ^{13}C magnetization due to $^{13}C-^2H$ scalar coupling allowed to occur. Immediately after the ^{13}C 90_y pulse at point e the magnetization of interest is given by $I_zC_zD_z$, where I_z, C_z, and D_z denote the z components of proton, carbon, and deuterium magnetization from the $^{13}CH_2D$ group, respectively. In the case of T_1 measurements, relaxation of the triple spin term, $I_zC_zD_z$, occurs during the subsequent T delay. The $90_{\phi 5}90$ ^2H pulse pair preceding T, with the phase $\phi 5$ alternated in sign in concert with the receiver phase, is employed to ensure that magnetization present during the T delay is proportional to D_z. In contrast, for measurement of ^2H $T_{1\rho}$ values, the ^2H $90_{\phi 5}$ pulse establishes magnetization of the form $I_zC_zD_y$ which is subsequently spin locked by the application of the SL_y pulse for time T. After the relaxation period T, magnetization is returned to ^1H for detection by reversing the pathway described above.

The pulse scheme of Figure 1a is quite similar to experiments developed by Bax and co-workers for the measurement of long-range $^{13}C-^{13}C$ scalar couplings.[19] In the present case two- and three-bond $^{13}C-^{13}C$ scalar couplings (0−4 Hz) can give rise to additional terms of the form $I_zC_yC_x^1D_z$ (T_1) or $I_zC_yC_x^1D_y$ ($T_{1\rho}$) during T, where C_y and C_x^1 are the y and x components of magnetization from the methyl carbon (C) and the long-range coupled carbon (C^1), respectively. Application of gradient g5 eliminates the double quantum contributions to these terms but the zero quantum components are refocused into observable magnetization; these terms are undesirable since their relaxation properties may well be different from either $I_zC_zD_z$ (T_1) or $I_zC_zD_y$ ($T_{1\rho}$). The application of the selective $^{13}C^\alpha$ 90° carbon pulse at point d (phase $\phi 4$) ensures that terms arising from the three-bond methyl-C^α couplings in Ile or Leu residues do not refocus. To within experimental error, identical $T_{1\rho}$ and T_1 values were measured using experiments with and without this purging pulse indicating that the contributions from long-range couplings are small.

During the T period, relaxation of terms of the form $I_zC_zD_y$ ($T_{1\rho}$) or $I_zC_zD_z$ (T_1) is measured. As will be shown below, the relaxation of both terms is dominated by the deuterium quadrupolar interaction. However, in the case of the decay of the $I_zC_zD_z$ term, in particular, there is a small but measurable contribution to the relaxation from proton spin flips involving spin I and neighboring proton spins. Fortunately, such effects are easily taken into account by measurement of the relaxation rate of I_zC_z, as described in detail below, and it is possible to extract the relaxation rates of the deuteron, $1/T_1(D)$ and $1/T_{1\rho}(D)$, in an accurate manner. The Hamiltonian which gives rise to the relaxation of the terms $I_z^iC_zD_z$ or $I_z^iC_zD_y$ (where the superscript i has been added to distinguish the two proton spins i and j of the $^{13}CH_2D$ methyl) can be written as:

$$\mathcal{H} = \mathcal{H}^Q(D) + \mathcal{H}^D(CD) + \mathcal{H}^D(I^iD) + \mathcal{H}^D(I^jD) + \mathcal{H}^D(I^iC) + \mathcal{H}^D(I^jC) + \mathcal{H}^D(CC^1) + \mathcal{H}^D(I^iI^j) + \sum_{k\neq i,j} \mathcal{H}^D(I^iI^k) \quad (2)$$

where $\mathcal{H}^Q(D)$ is the quadrupolar Hamiltonian for spin D and $\mathcal{H}^D(AB)$ is the dipolar Hamiltonian describing the interaction between dipolar coupled spins A and B. In eq 2, D, C, I^i, and I^j are the $^{13}CH_2D$ methyl deuterium (D), carbon (C), and proton (I^i, I^j) spins, respectively, while C^1 is the carbon spin one-bond coupled to C. A similar Hamiltonian holds for $I_z^jC_zD_z$ and $I_z^jC_zD_y$, as well, and is obtained by interchanging the i and j superscripts in eq 2. Note that the last term in eq 2 includes a summation over all of the proton spins, I^k ($k \neq i, j$), which are dipolar coupled to spin I^i. A calculation shows that the relaxation of $I_z^iC_zD_z$ can be described by

$$\mathrm{d/d}T\, I_z^iC_zD_z = -\rho_i^L\, I_z^iC_zD_z - \sigma_{ij}\, I_z^jC_zD_z - \sum_{k\neq i,j} \sigma_{ik}\, I_z^kC_zD_z \quad (3)$$

which includes an autorelaxation term (ρ_i^L) as well as terms arising from cross relaxation between dipolar coupled proton spins. Note that other terms in the Hamiltonian $\mathcal{H}^D$ can also contribute to cross relaxation; however, the cross relaxation terms that arise from these interactions are much smaller than σ_{ij} and σ_{ik} (see discussion below) and have therefore been neglected.

The relative contribution of each term of eq 2 to the autorelaxation (ρ_i^L) of $I_z^iC_zD_z$ has been calculated and the results summarized as follows:

$$\mathcal{H}^Q(D): \quad {}^3/_{16}(e^2qQ/\hbar)^2[J(\omega_D) + 4J(2\omega_D)]$$

$$\mathcal{H}^D(CD): \quad \gamma_C{}^2\gamma_D{}^2\hbar^2/(4r_{CD}{}^6)[3J(\omega_D) + 12J(\omega_C) + 6J(\omega_C + \omega_D) + J(\omega_C - \omega_D)]$$

$$\mathcal{H}^D(I^iD): \quad \gamma_1{}^2\gamma_D{}^2\hbar^2/(4r_{1D}{}^6)[3J(\omega_D) + 12J(\omega_1) + 6J(\omega_1 + \omega_D) + J(\omega_1 - \omega_D)]$$

$$\mathcal{H}^D(I^jD): \quad \gamma_1{}^2\gamma_D{}^2\hbar^2/(4r_{1D}{}^6)[J(\omega_1 - \omega_D) + 3J(\omega_D) + 6J(\omega_1 + \omega_D)]$$

$$\mathcal{H}^D(I^iC): \quad \gamma_1{}^2\gamma_C{}^2\hbar^2/(4r_{1C}{}^6)[3J(\omega_1) + 3J(\omega_C)]$$

$$\mathcal{H}^D(I^jC): \quad \gamma_1{}^2\gamma_C{}^2\hbar^2/(4r_{1C}{}^6)[J(\omega_1 - \omega_C) + 3J(\omega_C) + 6J(\omega_1 + \omega_C)]$$

$$\mathcal{H}^D(CC^1): \quad \gamma_C{}^4\hbar^2/(4r_{CC}{}^6)[J(0) + 3J(\omega_C) + 6J(2\omega_C)]$$

$$\mathcal{H}^D(I^iI^j): \quad \gamma_1{}^4\hbar^2/(4r_{11}{}^6)[J(0) + 3J(\omega_1) + 6J(2\omega_1)]$$

$$\mathcal{H}^D(I^iI^k): \quad \gamma_1{}^4\hbar^2/(4\langle r_{11}{}^3\rangle^2)[J(0) + 3J(\omega_1) + 6J(2\omega_1)],\ k \neq i, j \quad (4.1)$$

where ρ_i^L is given by the sum of all of the terms on the right-hand side of eq 4.1. In addition, $\mathcal{H}^D(I^iI^j)$ and $\mathcal{H}^D(I^iI^k)$ establish cross terms, σ_{ij} and σ_{ik}, respectively, which couple $I_z^iC_zD_z$ to

(19) Bax, A.; Vuister, G. W.; Grzesiek, S.; Delaglio, F.; Wang, A. C.; Tschudin, R.; Zhu, G. *Meth. Enzymol.* **1994**, *239*, 79.

$I_z^j C_z D_z$ and $I_z^k C_z D_z$. The cross relaxation terms indicated in eq 3 are given by

$$\sigma_{ij} = \gamma_1^4\hbar^2/(4r_{11}^6)[-J(0) + 6J(2\omega_1)] \quad (4.2)$$

$$\sigma_{ik} = \gamma_1^4\hbar^2/(4\langle r_{11}^3\rangle^2)[-J(0) + 6J(2\omega_1)]$$

In eq 4 e^2qQ/h is the quadrupolar coupling constant, γ_q is the gyromagnetic ratio of spin q, h is Planck's constant ($\hbar = h/(2\pi)$), r_{ij} is the distance between spins i and j, $\langle r\rangle$ is the time average of r and $J(\omega)$ is a spectral density function, defined below. It is understood that for each k in $\mathcal{H}^D(I^iI^k)$, r_{11} and the values of $J(\omega)$ in the final expressions in eqs 4.1 and 4.2 will change accordingly.

Noting that proton spins i and j are equivalent, it is straightforward to write analogous expressions for the decay of $I_z^j C_z D_z$ simply by interchanging i and j in the equations above. It is easily shown that

$$\mathrm{d/d}T\, I_zC_zD_z = -\{1/T_1(I_zC_zD_z)\}I_zC_zD_z - \sum_{k\neq i,j}(\sigma_{ik} + \sigma_{jk})I_z^kC_zD_z \quad (5)$$

where $I_z = I_z^i + I_z^j$, $1/T_1(I_zC_zD_z) = \rho^L + \sigma$, $\rho^L = \rho_i^L = \rho_j^L$, $\sigma = \sigma_{ij}$. The rapid rotation of the methyl group about its symmetry axis ensures that $\sigma_{ik} = \sigma_{jk}$.

The discussion above has focused on the relaxation of $I_zC_zD_z$. It is possible to derive similar equations for the relaxation of $I_zC_zD_y$. The evolution of $I_z^iC_zD_y$ is described according to eq 6,

$$\mathrm{d/d}T\, I_z^iC_zD_y = -\rho_i^T I_z^iC_zD_y - \sigma_{ij} I_z^jC_zD_y - \sum_{k\neq i,j}\sigma_{ik} I_z^kC_zD_y \quad (6)$$

where, as before, only the dominant cross relaxation terms due to $^1H-^1H$ dipolar interactions have been included. The contributions to ρ_i^T from the terms in eq 2 are given by

$\mathcal{H}^Q(D)$: $^1/_{32}(e^2qQ/\hbar)^2[9J(0) + 15J(\omega_D) + 6J(2\omega_D)]$

$\mathcal{H}^D(CD)$: $\gamma_C^2\gamma_D^2\hbar^2/(8r_{CD}^6)[4J(0) + 5J(\omega_C - \omega_D) + 3J(\omega_D) + 6J(\omega_C) + 30J(\omega_C + \omega_D)]$

$\mathcal{H}^D(I^iD)$: $\gamma_1^2\gamma_D^2\hbar^2/(8r_{1D}^6)[4J(0) + 5J(\omega_1 - \omega_D) + 3J(\omega_D) + 6J(\omega_1) + 30J(\omega_1 + \omega_D)]$

$\mathcal{H}^D(I^jD)$: $\gamma_1^2\gamma_D^2\hbar^2/(8r_{1D}^6)[4J(0) + J(\omega_1 - \omega_D) + 3J(\omega_D) + 6J(\omega_1) + 6J(\omega_1 + \omega_D)]$

$\mathcal{H}^D(I^jC)$: $\gamma_1^2\gamma_C^2\hbar^2/(4r_{1C}^6)[3J(\omega_1) + 3J(\omega_C)]$

$\mathcal{H}^D(I^jC)$: $\gamma_1^2\gamma_C^2\hbar^2/(4r_{1C}^6)[J(\omega_1 - \omega_C) + 3J(\omega_C) + 6J(\omega_1 + \omega_C)]$

$\mathcal{H}^D(CC^1)$: $\gamma_C^4\hbar^2/(4r_{CC}^6)[J(0) + 3J(\omega_C) + 6J(2\omega_C)]$

$\mathcal{H}^D(I^jI^j)$: $\gamma_1^4\hbar^2/(4r_{11}^6)[J(0) + 3J(\omega_1) + 6J(2\omega_1)]$

$\mathcal{H}^D(I^jI^k)$: $\gamma_1^4\hbar^2/(4\langle r_{11}^3\rangle^2)[J(0) + 3J(\omega_1) + 6J(2\omega_1)]$, $k \neq i, j$ (7)

The values for the cross relaxation rates, σ_{ij} and σ_{ik}, in eq 6 are indicated in eq 4.2. Because proton spins i and j are equivalent, it is convenient to recast eq 6 as

$$\mathrm{d/d}T\, I_zC_zD_y = -\{1/T_{1\rho}(I_zC_zD_y)\}I_zC_zD_y - \sum_{k\neq i,j}(\sigma_{ik} + \sigma_{jk})\, I_z^kC_zD_y \quad (8)$$

where $I_z = I_z^i + I_z^j$, $1/T_{1\rho}(I_zC_zD_y) = \rho^T + \sigma$, $\rho^T = \rho_i^T = \rho_j^T$, $\sigma = \sigma_{ij}$.

A number of different spectral density functions have been developed to interpret methyl relaxation data in the context of particular models of motion. In the discussion that follows, including the analysis of the relaxation data on PLCC SH2, we have chosen a particularly simple form of the spectral density function, $J(\omega)$, developed by Lapari and Szabo[20]

$$J(\omega) = 2/5[S^2\tau_m/(1 + (\omega\tau_m)^2) + (1 - S^2)\tau/(1 + (\omega\tau)^2)] \quad (9)$$

where τ_m is the overall correlation time for isotropic rotation, $\tau^{-1} = \tau_m^{-1} + \tau_e^{-1}$ where τ_e is the effective correlation time describing the internal motions, and the order parameter, S, is given by $S = S_{axis}[(3\cos^2\theta_1 - 1)/2]$. The factor $(3\cos^2\theta_1 - 1)/2$ takes into account the rapid rotation of the methyl group about its averaging axis. In the case of dipolar interactions, θ_1 is the angle between the dipole vector and the averaging axis, while for the quadrupolar terms θ_1 is the angle between the C−D bond and the averaging axis. For example, $\theta_1 = 109.5°$, 90°, and 0° in the expressions for relaxation originating from the Hamiltonians $\mathcal{H}^Q(D)$, $\mathcal{H}^D(I^iD)$, and $\mathcal{H}^D(CC^1)$, respectively. Finally, S_{axis} is the order parameter describing the motion of the averaging axis, assumed to be the bond vector connecting the methyl carbon and its adjacent carbon. More complex forms for the spectral density function can be assumed (see for example eq 6 of ref 21). However the values of S_{axis} are relatively insensitive to the form of $J(\omega)$ employed and we have used eq 9 in what follows; none of the conclusions in the present paper are affected by the specific choice of $J(\omega)$.

The contributions of each of the terms in eq 2 can be evaluated using eqs 4, 7, and 9 assuming explicit values for the various correlation times and order parameters. Of course, the contributions from $\mathcal{H}^D(I^iI^k)$, $k \neq i, j$, will depend on the number of proton spins I^k, the distance between spins I^i and I^k, as well as the exact details of the motion of the $I^i - I^k$ internuclear vectors. In what follows we consider the contribution from a single spin I^k, positioned along the 3-fold averaging axis of the methyl group at a distance of 2 Å from the methyl carbon. Our choice of a 2-Å distance is based on calculations of the effective distance, r_{eff} ($1/r_{eff} = [\sum 1/r^6]^{1/6}$), between a methyl carbon and a proton (not part of the methyl group in question) in a 50% random deuterated sample of the PLCC SH2−peptide complex. Preliminary results based on the present study involving the PLCC SH2 domain and a study of the dynamics of leucine methyl groups in the protein staphylococcal nuclease[21] suggest that $S_{axis}^2 = 0.5$ and $\tau_e = 35$ ps are reasonable values describing methyl dynamics in proteins. Assuming $\tau_m = 10$ ns, $S_{axis}^2 = 0.5$ and $\tau_e = 35$ ps, the contributions to the autorelaxation rate of $I_zC_zD_z$ ($1/T_1(I_zC_zD_z)$, eq 5) from the quadrupolar interaction, the proton−carbon dipolar $\{\mathcal{H}^D(IC),\ I = I^i + I^j\}$, and the proton−proton dipolar interactions $\{\mathcal{H}^D(I^iI^j) + \mathcal{H}^D(II^k),\ I = I^i + I^j\}$ are in the ratio 1.0:0.07:0.19, respectively. The other interactions described above make smaller contributions. Clearly, the largest contribution to the autorelaxation of the 3-spin order

(20) (a) Lipari, G.; Szabo, A. *J. Am. Chem. Soc.* **1982**, *104*, 4546. (b) Lipari, G.; Szabo, A. *J. Am. Chem. Soc.* **1982**, *104*, 4559.

(21) Nicholson, L. K.; Kay, L. E.; Baldisseri, D. M.; Arango, J.; Young, P. E.; Bax, A.; Torchia, D. A. *Biochemistry* **1992**, *31*, 5253.

term, other than the dominant quadrupolar term, arises from $^1H-^1H$ relaxation and such contributions must be measured accurately in order to obtain the correct value of $1/T_1(D)$. In a similar fashion, the contributions to the autorelaxation of $I_zC_zD_y$ ($1/T_{1\rho}(I_zC_zD_y)$, eq 8) can be evaluated and the same interactions described above dominate the relaxation rate. The ratio of the contributions to the autodecay rate are 1.0:0.01:0.04 for the quadrupolar, the proton−carbon dipolar, and the proton−proton dipolar interactions, respectively. The effects of the cross relaxation terms in eqs 5 and 8 have also been investigated for the case of $\tau_m = 10$ ns, $S_{axis}^2 = 0.5$ and $\tau_e = 35$ ps assuming a single proton, I^k, at a distance of 2 Å along the methyl averaging axis as before. It has also been assumed that the autorelaxation rates of the terms $I^k_zC_zD_z$ and $I^k_zC_zD_y$ differ from the autorelaxation rates of $I_zD_zD_z$ and $I_zC_zD_y$ ($I_z = I_z^i + I_z^j$) only in that an additional methyl proton I^k dipolar contribution is included in the description of the relaxation of $I^k_zC_zD_z$ and $I^k_zC_zD_y$. (Note that proton I^k is relaxated by both methyl proton spins of the $^{13}CH_2D$ group, while the methyl protons are relaxed by only single proton, I^k.) For relaxation times measured from decay curves extending to 1.5× the autodecay time, simulations establish that neglect of the second term in eq 5 (i.e., the term proportional to $\sigma_{ik} + \sigma_{jk}$) changes the calculated decay rate of $I_zC_zD_z$ by less than 1% while a change in the decay of $I_zC_zD_y$ of less than 0.1% is calculated when this term is neglected in eq 8. In fact, even for $\tau_m = 20$ ns ($S_{axis}^2 = 0.5$ and $\tau_e = 35$ ps) neglect of these terms changes the decay rates of $I_zC_zD_z$ and $I_zC_zD_y$ by less than 4% and by less than 0.1%, respectively.

The contributions from the $^1H-^1H$ dipolar interactions can be measured in a very straightforward manner from the decay rate of the 2-spin order term,[22] I_zC_z. In addition, the decay of I_zC_z also includes contributions from many of the other interactions which influence the relaxation of either $I_zC_zD_z$ or $I_zC_zD_y$. It is straightforward to show that, in the absence of cross correlation,

$$1/T_1(I_zC_zD_z) - 1/T_1(I_zC_z) = 1/T_1(D) + \delta 1$$

$$1/T_{1\rho}(I_zC_zD_y) - 1/T_1(I_zC_z) = 1/T_{1\rho}(D) + \delta 2 \quad (10.1)$$

where

$$1/T_1(D) = {}^3/_{16}(e^2qQ/\hbar)^2[J(\omega_D) + 4J(2\omega_D)] \quad (10.2)$$

$$1/T_{1\rho}(D) = {}^1/_{32}(e^2qQ/\hbar)^2[9J(0) + 15J(\omega_D) + 6J(2\omega_D)]$$

Simulations have established that for the spin lock fields employed in the present study (~1 kHz) and for the chemical shift range of methyl deuterons, $1/T_{1\rho}(D) = 1/T_2(D)$. Note that for all values of τ_m, S_{axis}^2, and τ_e examined ($3 \le \tau_m \le 25$ ns, $0.1 \le S_{axis}^2 \le 1$, $0 \le \tau_e \le 150$ ps) $\delta 1$ and $\delta 2$ make contributions of less than 2.5% to either $1/T_1(D)$ or $1/T_{1\rho}(D)$, respectively, and can therefore be neglected.[23]

Figure 1b illustrates one of several pulse schemes that can be employed to measure the decay of I_zC_z. Note that for this experiment it is not necessary to apply a $^{13}C^\alpha$ selective pulse (shaped pulse at point d in the sequence of Figure 1a) since in this case magnetization arising from long-range methyl−carbon homonuclear couplings is not refocused into observable signal by the remaining portion of the pulse scheme.

To this point in the discussion of the relaxation of $I_zC_zD_z$ and $I_zC_zD_y$, the effects of cross correlation between the various relaxation mechanisms listed in eq 2 have not been considered. In the discussion that follows we focus on correlations between the quadrupolar interaction and the C−D, I^i−D, and I^j−D dipolar interactions. A subsequent paper describes cross correlation and cross relaxation effects in greater detail and establishes rigorously that eq 10 with $\delta 1 = \delta 2 = 0$ is accurate.[23] The relative magnitudes of the contributions to relaxation from the deuterium quadrupolar interaction and the C−D and I−D dipolar interactions suggest that cross correlation effects should be very small. For example, for 3 ns $\le \tau_m \le$ 30 ns, $S_{axis}^2 = 0.5$, and $\tau_e = 0$ the contribution to the $1/T_1$ or $1/T_{1\rho}$ relaxation rate of a deuteron from the quadrupolar interaction is ≥500-fold higher than the contribution to the rate from a given C−D or I−D dipolar interaction. As the value of τ_e increases from zero the quadrupolar term dominates to an even greater extent. Consider the transverse relaxation of a deuteron (undergoing free precession) coupled to two protons, as is the case in a CH_2D group. The dominant terms in the quadrupolar and dipolar Hamiltonians contributing to the relaxation of D_{TR} are[24]

$$\mathcal{H}^Q(D) = A(e^2qQ/4\hbar)[(3\cos^2\theta_1 - 1)/2]3(D_z^2 - D\cdot D/3) = 3K_q(D_z^2 - D\cdot D/3)$$

$$\mathcal{H}^D(ID) = -A(\hbar\gamma_I\gamma_D/r_{ID}^3)[(3\cos^2\theta_2 - 1)/2]2I_zD_z = -2K_dI_zD_z \quad (11)$$

where all constants are defined as above, D_{TR} is transverse deuterium magnetization, $A = [(3\cos^2\theta - 1)/2]$, where θ is the angle between the averaging axis and the external magnetic field, θ_1 and θ_2 are the angles between the averaging axis and the C−D bond and the ID dipole vector, respectively ($\theta_1 = 109.5°$; $\theta_2 = 90°$), and I_z, and D_z are proton and deuterium spin operators, respectively. In eq 11 it has been assumed that the methyl group rotates much more rapidly about its symmetry axis than the rate of molecular tumbling. For clarity, we focus on the transitions $|0\,\alpha\,\alpha\rangle \rightarrow |1\,\alpha\,\alpha\rangle$ and $|0\,\beta\,\beta\rangle \rightarrow |1\,\beta\,\beta\rangle$ and we note that in $|A\,B\,C\rangle$, A is the spin state of the deuteron, while B and C denote the spin states of the two methyl protons. The transitions described above contribute to the outer (downfield) and inner (upfield) lines of the deuterium multiplet. The effect of $\mathcal{H} = \mathcal{H}^Q(D) + \mathcal{H}^D(ID)$ is to change the energies of the transitions $|0\,\alpha\,\alpha\rangle \rightarrow |1\,\alpha\,\alpha\rangle$ and $|0\,\beta\,\beta\rangle \rightarrow |1\,\beta\,\beta\rangle$, by the amounts $3K_q - 2K_d$ and $3K_q + 2K_d$, respectively. Since the contributions to the transverse relaxation rates of the multiplet components are proportional to the square of the energy shift,[22] a straightforward calculation shows that the relaxation rates of transverse magnetization corresponding to these two transitions differ by a factor of 1.4. Simulations for relaxation measurements extending in time T (see Figure 1) to a factor of 1.5× the relaxation time establish that this difference translates into errors in measured relaxation rates of less than 2%. The errors associated with cross correlation effects arising from interference between the quadrupolar and the C−D dipolar interactions are even smaller. Correspondingly small errors (<2.5%) are calculated for the effects of cross correlation on measured T_1 values. In principle, these small effects can be attenuated by the introduction of ^1H and ^{13}C 180° pulses during the period T. This is similar to what has previously been suggested for the elimination of cross correlation effects between the $^{15}N-^1H$ dipolar and the ^{15}N chemical shift anisotropy interactions in ^{15}N relaxation experiments.[22,25] In practice, however, imperfections in the pulses will lead to attenuation of the signal since in this case it is the decay of the 3-spin terms, $I_zC_zD_z$ and $I_zC_zD_y$,

(22) Kay, L. E.; Nicholson, L. K.; Delaglio, F.; Bax, A.; Torchia, D. A. *J. Magn. Reson.* **1992**, *97*, 359.

(23) Yang, D.; Kay, L. E. *J. Magn. Reson.* Submitted for publication.

(24) Abragam, A. *Principles of Nuclear Magnetism*; Clarendon Press, Oxford, 1961; Chapter VIII, p 289.

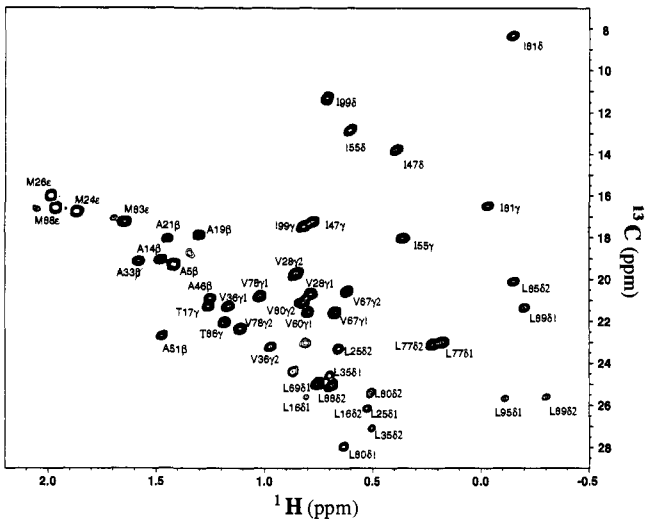

Figure 2. 2D contour plot of the constant time (^{13}C,^1H) spectrum of the C-terminal SH2 domain from phospholipase $C_{\gamma 1}$ recorded at 600 MHz. Only signals from CH_2D groups are observed. 76 complex t_1 points were acquired, with acquisition times of 13.8 and 64.0 ms in t_1 and t_2, respectively. The pulse scheme of Figure 1a was employed with a value of $T = 50$ μs. The stereospecific assignments of the methyl groups are listed and were obtained using the method of Neri *et al.*[34] A small amount of sample degradation has occurred giving rise to a number of extra weak peaks.

rather than D_z or D_y that is measured during T in the experiments of Figure 1a. Finally it should be noted that in the case of relaxation measurements involving $I_zC_zD_y$ described herein, a spin lock field is employed. Providing that the spin lock field is sufficiently strong so that the deuterium magnetization is locked in the transverse plane, it can be shown that the terms which give rise to quadrupolar–dipolar cross correlation become non-secular and the effect is, therefore, removed in $T_{1\rho}$ experiments.[23] Cross correlation effects between the various dipolar terms in eq 2 have also been calculated and contribute insignificantly to the measured decay rates of $I_zC_zD_z$ and $I_zC_zD_y$.[23]

Finally, it has not escaped our attention that it may be possible to obtain similar dynamics information from ^{13}C relaxation studies. This is particularly the case for fractionally deuterated, uniformly ^{13}C-labeled samples since the substitution of deuterons for protons can eliminate cross correlation effects between ^1H–^{13}C dipolar interactions which has proved to be a major problem in the analysis of carbon relaxation data from methyl groups.[26] Our laboratory has spent considerable effort in measuring carbon relaxation of methyls labeled as $^{13}CHD_2$, since in this case the carbon–proton spin pair can be treated effectively as an AX spin system. A number of serious problems have emerged with this method, however. First, reasonably strong scalar coupling between the C^γ and C^δ carbons of leucine residues complicates measurement of C^δ $T_{1\rho}$ values. In addition, (i) the elimination of two of the three methyl protons and (ii) the rapid rotation about the methyl symmetry axis which reduces the remaining ^1H–^{13}C dipolar interaction by a factor of 9 means that the relaxation of the methyl carbon can no longer be completely accounted for by including only contributions from directly bound spins. Simulations establish that for PLCC SH2, contributions to measured ^{13}C T_1 and $T_{1\rho}$ values from neighboring, nonbonded protons can be as large as 15–20%. Clearly it is difficult to account for such interactions in a completely quantitative fashion without both a very high resolution structure and knowledge of the relative motional properties of the spins involved. Finally, because the carbon relaxation properties depend on neighboring proton spins which may or may not be present from molecule to molecule as a result of the fractional deuteration scheme used to prepare the protein sample, the relaxation at a particular carbon site will be nonexponential. $T_{1\rho}$ experiments which select for methyls which are coupled to neighboring CD as opposed to CH groups show, on average, differences in relaxation times of approximately 5% relative to experiments which do not make such a selection. As an alternative to uniform ^{13}C labeling, fractional carbon labeling ensures that the effects of carbon coupling in carbon relaxation experiments are significantly attenuated.[27] However, this does not remove cross correlation between ^1H–^{13}C dipolar fields, and the sensitivity of experiments on such samples relative to those making use of full carbon labeling is reduced considerably.

The ^2H relaxation methods described above have been applied to study sidechain dynamics of PLCC SH2. Figure 2 shows a two-dimensional spectrum recorded at 600 MHz using the sequence of Figure 1a (T_1 sequence) with $T = 50$ μs. Well-resolved spectra displaying high sensitivity were obtained for both T_1 and $T_{1\rho}$ measurements. $T_1(I_zC_zD_z)$, $T_{1\rho}(I_zC_zD_y)$, and $T_1(I_zC_z)$ decay curves obtained for a number of the methyl groups in the protein are illustrated in Figure 3, demonstrating significant variations in dynamics at the different sites. The results of the present study are summarized in Figure 4 where $T_1(D)$, $T_{1\rho}(D)$, and $T_1(I_zC_z)$ values are plotted as a function of residue. The values of $T_1(D)$ and $T_{1\rho}(D)$ are obtained from measured relaxation rates using eq 10 with $\delta 1 = \delta 2 = 0$. With the exceptions of Leu 16δ2 and Leu 25δ1 which overlap completely, it is possible to measure rates for all of the methyl groups in the protein. In total relaxation properties for 45 of the 47 methyl groups have been measured. It is of particular interest to note that the $T_{1\rho}(D)$ values for Leu 69 and 77 are both significantly higher than for all of the other Leu residues suggesting increased mobility in this region. Note that S_{axis}^2 values of 0.20 are obtained for both Leu 69δ1 and δ2, and values of 0.28 and 0.25 are measured for Leu 77δ1 and δ2, respectively. In this context it is interesting to note that Leu 69 participates strongly in the binding of peptide, and shows a large number of NOE interactions with the proline three residues C-terminal to the phosphotyrosine of the peptide.[14] Also of interest is that Leu 69 and 77 have very low surface accessibilities in the complex of the PLCC SH2 domain with peptide. The variations in mobility as a function of residue are best

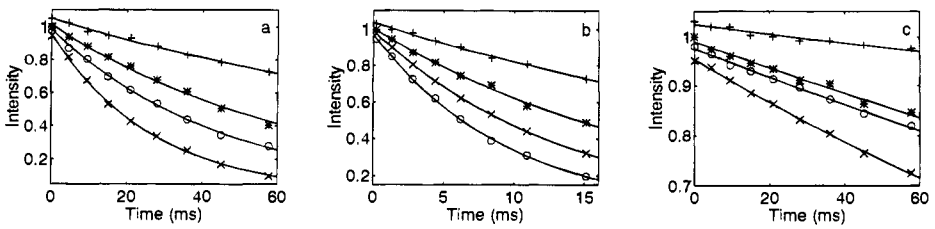

Figure 3. $T_1(I_zC_zD_z)$ (a), $T_{1\rho}(I_zC_zD_y)$ (b), and $T_1(I_zC_z)$ (c) decay curves for methyl groups of residues Ala 14 (O), Ile 99δ (*), Val 67γ2 (×), and Met 26 (+) obtained from the intensities of cross peaks in 2D spectra recorded at 600 MHz as a function of the delay time T. Several of the curves have been multiplied by different factors to aid in visualization.

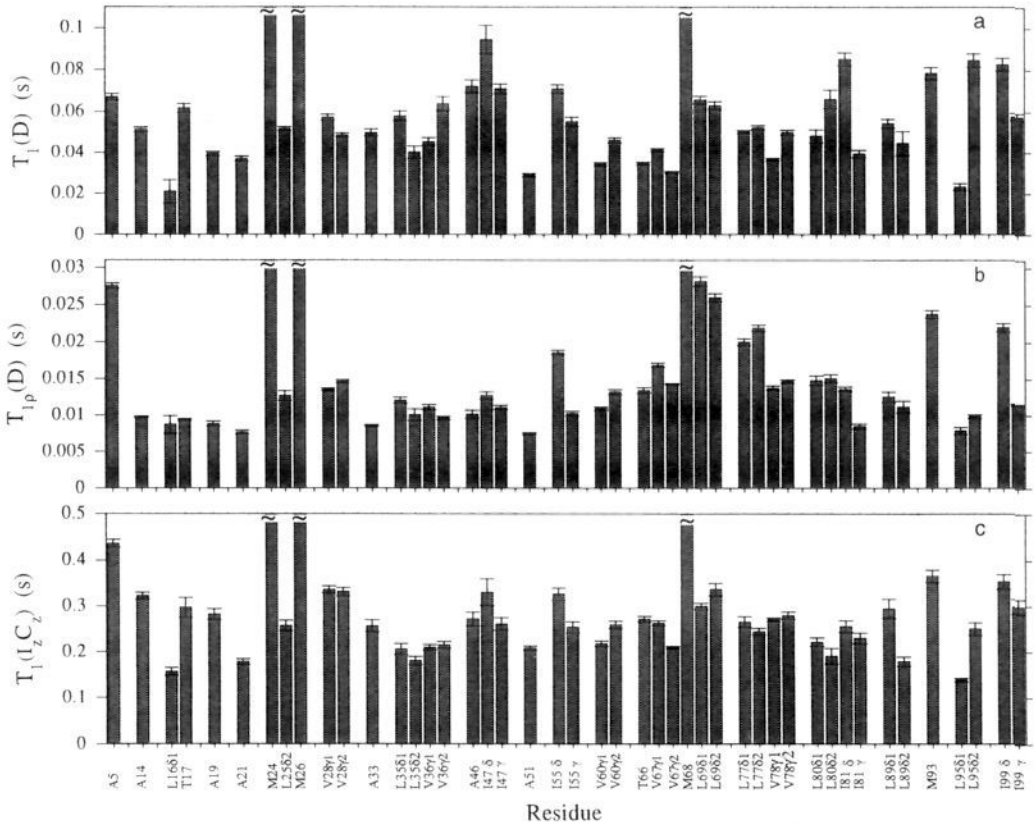

Figure 4. $T_1(D)$ (a), $T_{1\rho}(D)$ (b), and $T_1(I_zC_z)$ (c) values (600 MHz) for methyl groups of PLCC SH2 with errors in the measurements indicated for each residue. Leu 16δ2 and Leu 25δ1 overlap completely and relaxation times for these residues are therefore not available. The (small) contributions from the selective $1/T_1$ decay rates of spins I and C have been eliminated as described in the text. The $T_1(D)$, $T_{1\rho}(D)$, and $T_1(I_zC_z)$ values for Met 24, 26, and 68 are off-scale; the values are (0.155 ± 0.007, 0.039 ± 0.001, 0.670 ± 0.032), (0.184 ± 0.007, 0.044 ± 0.001, 1.095 ± 0.101), and (0.176 ± 0.005, 0.054 ± 0.002, 0.877 ± 0.051) for Met 24, 26, and 68, respectively.

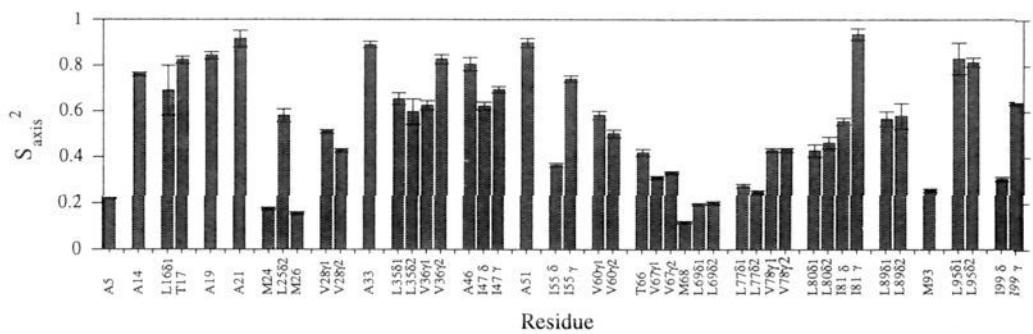

Figure 5. S_{axis}^2 vs residue for methyl groups of PLCC. Dynamic parameters can be extracted from $1/T_{1\rho}(D)$ and $1/T_1(D)$ values using a value of 165 kHz for the ^{2}H quadrupole coupling constant e^2qQ/h.[35] The equation relating $1/T_{1\rho}(D)$ to spectral densities, $J(\omega)$, is a complicated function of $\theta = \tan^{-1}(\omega_1/\Delta\omega)$ where ω_1 is the spin lock field and $\Delta\omega$ is the offset from the carrier. The exact expression is given by eq 12 of ref 36 with $K = (3/16)(e^2qQ/\hbar)^2$ and $J(\omega)$ defined by eq 9 of the present paper. Simulations show that for the spin lock fields employed in this study and the chemical shift range of methyl deuterons, the assumption $1/T_{1\rho}(D) = 1/T_2(D)$ is valid (i.e., $1/T_{1\rho}(D) = {}^1/_{32}(e^2qQ/\hbar)^2[\,9J(0) + 15J(\omega_D) + 6J(2\omega_D)]$; $1/T_1(D) = {}^3/_{16}(e^2qQ/\hbar)^2[J(\omega_D) + 4J(2\omega_D)]$. A value of $\tau_m = 7.7$ ns has been employed, based on ^{15}N T_1, T_2, and ^{1}H−^{15}N relaxation measurements performed on the same sample used for ^{2}H relaxation studies.

illustrated in Figure 5 which shows the values of S_{axis}^2 calculated from $T_1(D)$ and $T_{1\rho}(D)$ values measured at both 500 and 600 MHz. Because our sample is also labeled with ^{15}N, the overall correlation time, τ_m, is estimated from ^{15}N T_1, T_2, and NOE measurements. The measured ^{2}H T_1 and $T_{1\rho}$ rates are sufficient, therefore, to allow extraction of S_{axis}^2 and τ_e values. Analysis of the values of S_{axis}^2 for methyl groups from different residues

(25) (a) Boyd, J.; Hommel, U.; Campbell, I. D. *Chem. Phys. Lett.* **1990**, *175*, 477. (b) Palmer, A. G.; Skelton, N. J.; Chazin, W. J.; Wright, P. E.; Rance, M. *Mol. Phys.* **1991**, *75*, 699.
(26) (a) Werbelow, L. G.; Grant, D. M. In *Advances in Magnetic Resonance;* Waugh, J. S., Ed.; Academic Press: San Diego, 1977; Vol. 9, p 189. (b) Kay, L. E.; Torchia, D. A. *J. Magn. Reson.* **1991**, *95*, 536.
(27) Wand, A. J.; Bieber, R. J.; Urbauer, J. L.; Mcevoy, R. P.; Zhehong, G. *J. Magn. Reson. Ser.* B **1995**, *108*, 173.
(28) Geen, H.; Freeman, R. *J. Magn. Reson.* **1991**, *93*, 93.
(29) Boyd, J.; Scoffe, N. *J. Magn. Reson.* **1989**, *85*, 406.
(30) Patt, S. *J. Magn. Reson.* **1992**, *96*, 94.
(31) McCoy, M.; Mueller, L. *J. Am. Chem. Soc.* **1992**, *114*, 2108.
(32) Shaka, A. J.; Keeler, J.; Frenkiel, T.; Freeman, R. *J. Magn. Reson.* **1983**, *52*, 335.
(33) McCoy, M.; Mueller, L. *J. Magn. Reson.* **1992**, *98*, 674.
(34) Neri, D.; Szyperski, T.; Otting, G.; Senn, H.; Wuthrich, K. *Biochemistry* **1988**, *28*, 7510.
(35) Burnett, L. H.; Muller, B. H. *J. Chem. Phys.* **1971**, *55*, 5829.
(36) Jones, G. P. *Phys. Rev.* **1966**, *148*, 332.

indicates that while, on average, alanine residues have the largest S_{axis}^2 values and methionine methyls have the lowest order parameters, a lack of any appreciable correlation between mobility and sidechain length is observed for the other amino acids. In this regard it is clear that differential sidechain dynamics are significant. For example, for Leu 95δ1 and δ2 methyl groups, S_{axis}^2 values of 0.83 and 0.81 are obtained. In contrast, significantly lower values of 0.31 and 0.33 are measured for Val 67 γ1 and γ2, respectively, despite the fact that the sidechain length is somewhat smaller for valine relative to leucine residues. A correlation between surface accessibility and sidechain dynamics has not been observed in the present study. We are currently in the process of recording data on the complex to investigate how the dynamics change upon peptide binding. A more detailed analysis of the relaxation data and motional parameters will follow.

In summary, we have presented experiments for measuring dynamics of methyl groups via measurement of ^2H T_1 and $T_{1\rho}$ relaxation times in proteins which are uniformly ^{13}C labeled and fractionally deuterated. A detailed description of the relaxation properties of CH_2D methyl groups has been presented to establish that accurate values of deuterium relaxation rates, $1/T_1(D)$ and $1/T_{1\rho}(D)$, can be measured. The experiments are of high sensitivity and straightforward to use, and because the quadrupolar interaction dominates the relaxation of the deuteron, interpretation of the relaxation data is more straightforward than is the case for relaxation data from other nuclei, where the relaxation rates often contain contributions from several interactions. We are applying the methodology described to study sidechain dynamics in both the free and bound states of the SH2 domain of PLCC, where the measured relaxation times demonstrate significant variability in motion at different sidechain positions in the molecule.

Acknowledgment. The authors are grateful to Drs. Debbie Mattiello and Steve Smallcombe, Varian, for helpful comments regarding disabling of the lock receiver, Randall Willis for preparing the PLCC SH2 sample, and Dr. Dennis Torchia for very helpful discussions. This research was supported by the National Cancer Institute of Canada, the Natural Sciences and Engineering Research Council of Canada, and the Protein Engineering Network Centers of Excellence. T. Y. was the recipient of a Human Frontiers Science Program Fellowship.

Note Added in Proof: We have noted that in all experiments that employ ^2H decoupling improved lock stability can be achieved by ensuring that saturation and dephasing of ^2H spins during the pulse scheme is minimized and that ^2H magnetization is restored to the $+Z$ axis prior to enabling the lock receiver. Therefore, where ^2H decoupling is applied (WALTZ-16 sequence with pulses of phase $\pm x$), the decoupling element is sandwiched between a ^2H 90_y, 90_{-y} pulse pair (i.e., 90_y–$WALTZ_x$–90_{-y}) in a manner completely analogous to the procedure employed for minimizing water saturation and dephasing when ^1H decoupling is applied during an experiment recorded on an H_2O sample.[37] In the sequences of Figures 1 and 6, where ^2H pulses are phase cycled (ϕ5 and ϕ4 in Figures 1 and 6, respectively), the ^2H pulses sandwiching one of the decoupling elements must be cycled to ensure that deuterium magnetization is placed along $+Z$ prior to enabling of the lock. Farmer and Venters have also made use of such a scheme for ^2H decoupling.[3]

(37) Kay, L. E.; Xu, G. Y.; Yamazaki, T. *J. Magn. Reson.* **1994**, *A109*, 129.

Appendix I: Choice of $^{13}CH_2D$ Methyl Groups for Dynamics Studies

The use of a (semi-) random deuteration approach (see Experimental Section) to generate a fractionally labeled sample provides methyl groups at all levels of deuteration (i.e.: CH_3, CH_2D, CHD_2, and CD_3). It may appear, at first glance, that the methodology developed would work equally well for both $^{13}CHD_2$ and $^{13}CH_2D$ groups. In fact, we prefer to measure the relaxation properties of $^{13}CH_2D$ methyls. Our choice can be understood by considering the evolution of carbon magnetization during the τ_c delay indicated in Figures 1a,b. Recognizing that in a CD spin system the three lines of the carbon triplet can be represented as

$$\begin{aligned} &C_x(1 - D_z^2), && \text{center line} \\ &0.5C_x(D_z^2 + D_z), && \text{outer line} \\ &0.5C_x(D_z^2 - D_z), && \text{inner line} \end{aligned} \tag{12}$$

allows one to write the evolution of C_x due to C–D scalar coupling as

$$C_x \rightarrow C_x(1 - D_z^2) + C_xD_z^2 \cos(2\pi J_{CD}\tau_c) + C_yD_z \sin(2\pi J_{CD}\tau_c) \tag{13}$$

Note that the sum of the inner and outer lines of the triplet is given by $C_xD_z^2$ and that only these two lines evolve due to scalar coupling. For $\tau_c = 1/(4J_{CD})$, two-thirds of the carbon magnetization in a C–D spin system can be transferred to the deuteron in the absence of relaxation.

For the case of a $C-D_2$ spin system the evolution is more complex since the carbon multiplet is now a 1:2:3:2:1 pentet. It can be shown that $C_x \rightarrow A1 + A2 + A3 + A4$ where

$$\begin{aligned} A1 = {} & C_x(1 - D_{z,1}^2)(1 - D_{z,2}^2) + \\ & 0.25C_x(D_{z,1}^2 + D_{z,1})(D_{z,2}^2 - D_{z,2}) + \\ & 0.25C_x(D_{z,1}^2 - D_{z,1})(D_{z,2}^2 + D_{z,2}) \end{aligned}$$

$$\begin{aligned} A2 = {} & C_x(1 - D_{z,1}^2)D_{z,2}^2 \cos(2\pi J_{CD}\tau_c) + \\ & C_y(1 - D_{z,1}^2)D_{z,2} \sin(2\pi J_{CD}\tau_c) \end{aligned}$$

$$\begin{aligned} A3 = {} & C_xD_{z,1}^2(1 - D_{z,2}^2) \cos(2\pi J_{CD}\tau_c) + \\ & C_yD_{z,1}(1 - D_{z,2}^2) \sin(2\pi J_{CD}\tau_c) \end{aligned}$$

$$\begin{aligned} A4 = {} & [0.25C_x(D_{z,1}^2 + D_{z,1})(D_{z,2}^2 + D_{z,2}) + \\ & 0.25C_x(D_{z,1}^2 - D_{z,1})(D_{z,2}^2 - D_{z,2})] \cos(4\pi J_{CD}\tau_c) + \\ & [0.25C_y(D_{z,1}^2 + D_{z,1})(D_{z,2}^2 + D_{z,2}) - \\ & 0.25C_y(D_{z,1}^2 - D_{z,1})(D_{z,2}^2 - D_{z,2})] \sin(4\pi J_{CD}\tau_c) \end{aligned} \tag{14}$$

In eq 14 $D_{z,1}$ and $D_{z,2}$ denote the z components of D magnetization associated with deuterons 1 and 2, respectively. The three terms in A1 correspond to carbon magnetization coupled to deuterons 1 and 2 with magnetic quantum number, (m_1), values of (0,0), (1,−1), and (−1,1), respectively. In direct analogy to the first term in eq 13 none of these terms evolve under scalar coupling. Terms A2 and A3 describe the evolution of C_x coupled to deuterons with m_1 values of (0,±1) or (±1,0), respectively. Note that these terms evolve in an analogous fashion to the second and third terms in eq 13. Finally, A4 corresponds to the evolution of transverse x carbon magnetization due to coupling with deuterons having m_1 values of

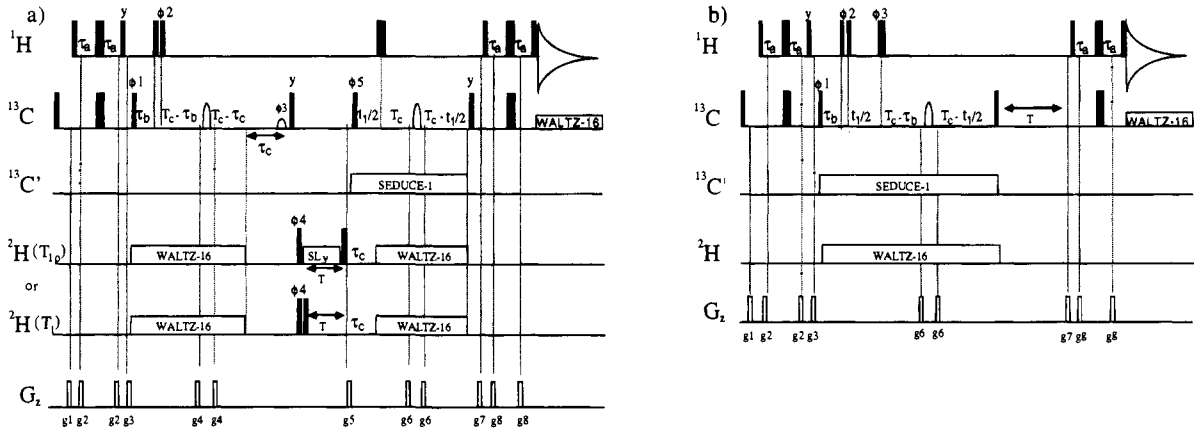

Figure 6. (a) Pulse schemes to measure $T_{1\rho}(I_zC_zD_y)$ or $T_1(I_zC_zD_z)$ values in $^{13}CH_2D$ spin systems with improved resolution. Experimental details are described in Figure 1. The phase cycling used is as follows: $\phi1 = 8(x), 8(-x)$; $\phi2 = (x,-x)$; $\phi3 = 8(x), 8(-x)$; $\phi4 = 2(x), 2(-x)$; $\phi5 = 4(x), 4(-x)$; acq $= x, 2(-x), x, -x, 2(x), 2(-x), 2(x), -x, x, 2(-x)$,x. Quadrature in F_1 is achieved via States-TPPI[16] of $\phi5$. The gradients employed are as follows ($\phi2 = x$): g1 = (0.5 ms, 5 G/cm), g2 = (0.3 ms, 3 G/cm), g3 = (1.5 ms, 15 G/cm), g4 = (0.3 ms, −25 G/cm), g5 = (0.4 ms, −10 G/cm), g6 = (0.2 ms, 10 G/cm), g7 = (1.0 ms, 15 G/cm), g8 = (0.3 ms, 2G/cm). Gradients g4, g5, g6, and g7 are phase cycled with $\phi2$. (b) Pulse scheme to measure $T_1(I_zC_z)$ with improved resolution. Details of the experiment are described in the legend to Figure 1b with the exception that for $\phi2 = x$ all of the gradients are of the same sign and the signs of gradients g6 and g7 are phase cycled with $\phi2$.

$(\pm1,\pm1)$. Selecting for the component of magnetization proportional to C_y preserves the following terms during T ($^{13}CHD_2$ methyl group)

$$C_z(D_{z,1} + D_{z,2}) \sin(2\pi J_{CD}\tau_c) + [C_zD_{z,1}{}^2D_{z,2} + C_zD_{z,1}D_{z,2}{}^2][-\sin(2\pi J_{CD}\tau_c) + 0.5 \sin(4\pi J_{CD}\tau_c)] \quad (15.1)$$

for the T_1 experiment and terms obtained by substituting D_y for D_z in the case of the $T_{1\rho}$ experiment. In contrast a term of the form

$$C_zD_z \sin(2\pi J_{CD}\tau_c) \quad (15.2)$$

is obtained for a $^{13}CH_2D$ methyl. It is clear that the relaxation of the expression given by eq 15.1 is complex since terms proportional to both D_z and $D_{z,i}{}^2D_{z,j}$ are present for all values of τ_c and the relaxation properties of such terms may be quite different. In contrast to the case of $^{13}CHD_2$ methyls, the relaxation of magnetization originating from $^{13}CH_2D$ groups is much more straightforward since only terms proportional to D_z are present during the relaxation time, T. It is possible to select preferentially for the first term in eq 15.1 through the choice of a short value of τ_c, however this results in a compromise in the sensitivity of the experiments.

Appendix II: Pulse Schemes for Measurement of ^2H Relaxation Properties in $^{13}CH_2D$ Methyl Groups with Improved Resolution

In the pulse scheme of Figure 1a carbon chemical shift evolution occurs during the interval in which the selection of CH_2D methyl groups proceeds (i.e., during the first $2T_C$ period, between points b and e). This limits the acquisition time in t_1 to $2(\tau_c - \tau_b) \sim 14$ ms. It is possible to improve the resolution by recording the carbon chemical shift evolution during the second $2T_C$ interval, as illustrated in Figure 6a. Note that the selection of CH_2D methyls proceeds during the first $2T_C$ period, as before. Figure 6b illustrates a pulse sequence which measures the decay of I_zC_z magnetization, while providing improved resolution in the carbon dimension. For samples which are randomly and fractionally deuterated, resolution in the carbon dimension is limited by two- and three-bond ^2H isotope shifts; for this reason $t_1{}^{max}$ values of somewhat less than $2T_C$ are typically employed.

JA952025H